11-2020

LRRC8 family proteins within lysosomes regulate cellular osmoregulation and enhance cell survival to multiple physiological stresses

Ping Li

Meiqin Hu

Ce Wang

Xinghua Feng

ZhuangZhuang Zhao

See next page for additional authors

Recommended Citation

Li, P., Hu, M., Wang, C., Feng, X., Zhao, Z., Yang, Y., Sahoo, N., Gu, M., Yang, Y., Xiao, S., Sah, R., Cover, T. L., Chou, J., Geha, R., Benavides, F., Hume, R. I., & Xu, H. (2020). LRRC8 family proteins within lysosomes regulate cellular osmoregulation and enhance cell survival to multiple physiological stresses. Proceedings of the National Academy of Sciences, 117(46), 29155. https://doi.org/10.1073/pnas.2016539117

LRRC8 family proteins within lysosomes regulate cellular osmoregulation and enhance cell survival to multiple physiological stresses

Ping Li[a,b,1], Meiqin Hu[a,b,2], Ce Wang[a,2], Xinghua Feng[b], ZhuangZhuang Zhao[b], Ying Yang[a], Nirakar Sahoo[a,c], Mingxue Gu[a], Yexin Yang[a], Shiyu Xiao[a], Rajan Sah[d], Timothy L. Cover[e,f,g], Janet Chou[h], Raif Geha[h], Fernando Benavides[i], Richard I. Hume[a,1], and Haoxing Xu[a]

[a]Department of Molecular, Cellular, and Developmental Biology, The University of Michigan, Ann Arbor, MI 48109-1085; [b]Collaborative Innovation Center of Yangtze River Delta Region Green Pharmaceuticals, College of Pharmaceutical Sciences, Zhejiang University of Technology, 310014 Hangzhou, China; [c]Department of Biology, The University of Texas Rio Grande Valley, Edinburg, TX 78539-2999; [d]Center for Cardiovascular Research, Division of Cardiology, Department of Internal Medicine, Washington University School of Medicine, St. Louis, MO 63110; [e]Department of Medicine, Vanderbilt University School of Medicine, Nashville, TN 37212; [f]Department of Pathology, Microbiology and Immunology, Vanderbilt University School of Medicine, Nashville, TN 37212; [g]Veterans Affairs Tennessee Valley Healthcare System, Nashville, TN 37212; [h]Division of Immunology, Boston Children's Hospital, Boston, MA 02115; and [i]Department of Epigenetics and Molecular Carcinogenesis, The University of Texas MD Anderson Cancer Center, Smithville, TX 78957

Edited by Ardem Patapoutian, Scripps Research Institute, La Jolla, CA, and approved October 5, 2020 (received for review August 4, 2020)

LRRC8 family proteins on the plasma membrane play a critical role in cellular osmoregulation by forming volume-regulated anion channels (VRACs) necessary to prevent necrotic cell death. We demonstrate that intracellular LRRC8 proteins acting within lysosomes also play an essential role in cellular osmoregulation. LRRC8 proteins on lysosome membranes generate large lysosomal volume-regulated anion channel (Lyso-VRAC) currents in response to low cytoplasmic ionic strength conditions. When a double-leucine $L^{706}L^{707}$ motif at the C terminus of LRRC8A was mutated to alanines, normal plasma membrane VRAC currents were still observed, but Lyso-VRAC currents were absent. We used this targeting mutant, as well as pharmacological tools, to demonstrate that Lyso-VRAC currents are necessary for the formation of large lysosome-derived vacuoles, which store and then expel excess water to maintain cytosolic water homeostasis. Thus, Lyso-VRACs allow lysosomes of mammalian cells to act as the cell`s "bladder." When Lyso-VRAC current was selectively eliminated, the extent of necrotic cell death to sustained stress was greatly increased, not only in response to hypoosmotic stress, but also to hypoxic and hypothermic stresses. Thus Lyso-VRACs play an essential role in enabling cells to mount successful homeostatic responses to multiple stressors.

lysosome | osmoregulation | chloride channel | vacuolation | exocytosis

A fundamental aspect of cell physiology is that, when the extracellular osmolarity is raised or lowered from the normal level, water flows across the plasma membrane. This results in rapid changes in cell volume and would disrupt plasma membrane integrity and lead to cell death if compensatory mechanisms were not rapidly activated (1, 2). In mammals, organismal level mechanisms regulating salt and water balance ensure that most cell types probably never encounter large osmotic gradients like those frequently encountered by the cells lining the digestive tract and the collecting tubules of the kidney (3), but, nonetheless, cells from most or all tissues of mammals display rapid adaptations to both hypo- and hyperosmotic challenges (1, 2).

Cellular osmoregulation is pivotal for maintaining intracellular water homeostasis, cell volume, and membrane integrity under osmotic challenges (2, 4, 5). In circumstances of hyperosmolarity, water leaves the cell, leading to an excess of plasma membrane which has to be internalized to allow cellular volume shrinkage (6). Hypoosmolarity elicits a complementary process leading to cellular volume expansion. Excess membrane lipids stored in protrusions and invaginations, such as microvilli and caveolae, are used to successfully deal with the immediate volume increase in animal cells (6, 7). If hypoosmotic conditions persist after the folded area is used up, the insertion of intracellular membrane materials to the plasma membrane via exocytosis is required for cell surface tension reduction (8, 9). Additionally, in epithelial cells of the kidney, when luminal water in the collecting duct rushes through aquaporin channels on the apical membrane, intracellular giant vacuoles derived from endocytotic compartments are essential for cell osmoregulation (10, 11). These intracellular membrane trafficking and cytoplasmic structure changes under osmotic stress suggest that a contribution of intracellular organelles to cellular osmoregulation may exist (10). The lysosome has been referred to as the "osmometer" of mammalian cells (12) because it responds to the osmotic pressure (13), and lysosomes may be a source of intracellular lipids that are added to the plasma membrane under hypotonic condition (8, 9). However, the cellular and molecular basis of intracellular osmoregulatory mechanisms is poorly understood.

Volume-regulated anion channels (VRACs), which are composed of LRRC8 family proteins (LRRC8A to -E) assembled as hexamers, have been demonstrated to play an essential role in cellular osmoregulation (5, 14–16). Studies deleting and then

Significance

Cells encountering physiological stresses often become vacuolated, but the source of the vacuoles and their role in causing or ameliorating necrotic cell death are unclear. Studies of cells responding to hypoosmotic, hypoxic, or hypothermic stress revealed that 1) vacuoles are derived from lysosomes, 2) many vacuoles subsequently undergo exocytosis, and 3) blocking either vacuolation or vacuole exocytosis by genetic or pharmacological approaches led to greatly increased necrotic cell death. By storing and then expelling excess water, lysosome-derived vacuoles maintain cytosolic water homeostasis and relieve membrane stress. This basic cellular function was present in all mammalian cell types tested and required ionic strength-sensitive ion channels formed from LRRC8 proteins on lysosomal membranes (Lyso-VRACs) acting in parallel with plasma membrane VRAC channels.

Author contributions: P.L. and H.X. designed research; P.L., M.H., C.W., X.F., Z.Z., Ying Yang, N.S., M.G., Yexin Yang, and S.X. performed research; R.S., T.L.C., J.C., R.G., and F.B. contributed new reagents/analytic tools; P.L., M.H., C.W., X.F., R.I.H., and H.X. analyzed data; and P.L., R.I.H., and H.X. wrote the paper.

The authors declare no competing interest.

This article is a PNAS Direct Submission.

[1]To whom correspondence may be addressed. Email: pinglium@umich.edu or rhume@umich.edu.

[2]M.H. and C.W. contributed equally to this work.

This article contains supporting information online at https://www.pnas.org/lookup/suppl/doi:10.1073/pnas.2016539117/-/DCSupplemental.

First published November 2, 2020.

reexpressing the various LRRC8 genes indicate that detectable levels of VRAC channel function on the plasma membrane require LRRC8A (*Swell1*) and at least one other subunit, that the properties of the channels vary depending on whether the partner is LRRC8B, -C, -D, or -E, and that LRRC8A expressed alone at very high levels can form functional channels (15–17).

We used stimulated emission depletion (STED) microscopy and electrophysiological recordings from giant vacuoles to demonstrate that there is a substantial amount of expression of LRRC8 family members on lysosome membranes, and that these proteins form functional lysosomal volume-regulated anion channels (Lyso-VRACs). By genetically and pharmacologically

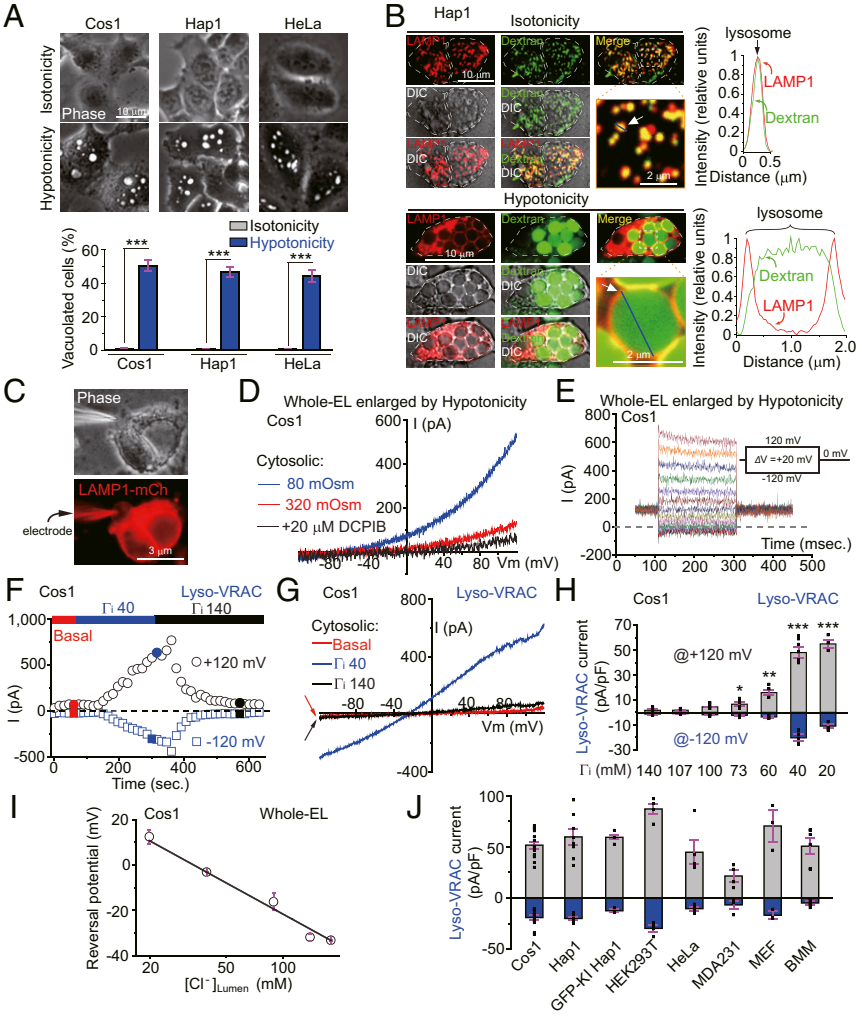

Fig. 1. Hypotonicity induces lysosome vacuolation and induces a chloride current in vacuoles. (*A*) Responses of Cos1, Hap1, and HeLa cells to a hypotonic challenge. Thirty minutes prior to data collection, the complete medium was replaced with fresh complete medium (Isotonicity, 300 mOsm) or the test medium (Hypotonicity, 170 mOsm). The photomicrographs show phase contrast images with examples of the vacuoles (bright white spots) commonly observed in cells exposed to hypotonic solutions. Also see Movie S1. The *Lower* quantifies data from many similar images with the parameter "Vacuolated Cell (%)," indicating the proportion of cells with at least one vacuole. In all panels with asterisks * is $P < 0.05$. ** is $P < 0.01$. *** is $P < 0.001$. (*B*) Each group of images shows cells studied after 0.5 h in either 300 mOsm (*Upper*) or 170 mOsm (*Lower*) medium. Each panel shows superimposed DIC (differential interference contrast) and fluorescence images. The red signal is LAMP1-mCherry driven by transient transfection, and the green signal is Dextran-Green loaded into the cell by endocytosis. The graph to the *Right* of each panel shows the fluorescence intensity of a line scan (blue line on the blown-up image) through the double labeled object indicated by the white arrow. (*C*) Images demonstrating the whole-endolysosome (whole-EL) patch-clamp configuration being achieved on a vacuolated lysosome that had been induced by hypotonic (80 mOsm) challenge. Note that approximately half the cell had been torn away to make the vacuole accessible for recording. See also *SI Appendix*, Fig. S2*A*. (*D* and *E*) Representative currents on vacuoles of Cos1 cells induced by exposure to 80 mOsm solution. The difference between the currents in 320 mOsm cytosolic solution and 80 mOsm cytosolic solution is defined as Lyso-VRAC. The currents in *D* were elicited by 200-ms ramps from −120 mV to +120 mV with the membrane potential (V_m) at each time point indicated on the *x* axis. The currents in *E* were elicited by voltage steps using the protocol shown to the right of the current traces. The dashed line indicates 0 pA. (*F*) The time course of cytosolic ionic strength effects on Lyso-VRAC currents at ±120 mV obtained from traces like those illustrated in *G*. (*G*) Representative I-V (current-voltage) traces from vacuoles of Cos1 cells treated with vacuolin in response to various cytosol-side solutions (Basal, 140 mM K-Gluconate, 290 mOsm; Γ_i 40, 40 mM CsCl, 290 mOsm; Γ_i 140, 140 mM CsCl, 290 mOsm). (*H*) Intracellular ionic strength (Γ_i) dependence of Lyso-VRAC. (*I*) Reversal potential of the Lyso-VRAC current was dependent on $[Cl^-]_{Lumen}$. The slope of the line fit to the data was −46.1 ± 0.5 mV per 10-fold concentration change. (*J*) $I_{Lyso\text{-}VRAC}$ induced by Γ_i 40 in additional cell types. In addition to Cos1, HeLa, and Hap1 cells, the cell types shown are Hap1 cells in which the endogenous *LRRC8A* gene was replaced with a sequence encoding an *LRRC8A*-GFP fusion protein (GFP-KI Hap1), HEK293T, human breast cancer cells (MDA231), mouse embryonic fibroblasts (MEF), and WT mouse bone marrow macrophages (BMM). For all panels showing averaged data, $n > 6$ and Student's *t* tests were used to determine statistical significance. pA, picoamperes; pF, picofarads.

selective manipulation of Lyso-VRAC activity, we demonstrate that both plasma membrane VRACs (PM-VRACs) and Lyso-VRACs are required to prevent necrotic cell death following hypoosmotic stress. Furthermore, Lyso-VRACs are also required to successfully respond to two other stresses that can lead to necrotic cell death.

Results

Lysosomes Are Highly Osmosensitive Organelles in Many Types of Mammalian Cells. Our initial studies of lysosomal responses to a hypoosmotic challenge focused on Cos1 cells (an epithelial cell line derived from the kidney of an African green monkey) because, in the kidney, the luminal osmolarity can range widely, from 50 milliosmolar (mOsm) to 1,200 mOsm, depending on the hydration state of the individual (18). Consistent with previous studies (10, 11, 19), Cos1 cells exposed to a physiologically relevant hypoosmotic challenge (170 mOsm rather than the normal 300 mOsm) demonstrated extensive cytoplasmic vacuolation 30 min after the solution change (Fig. 1*A*). Similar responses in about the same proportion of cells were observed in Hap1 cells (a leukemia-derived cell line) and HeLa cells (a cervical epithelial-derived cell line). Thus cytoplasmic vacuolation in response to hypotonicity is not limited to those mammalian cell types most likely to encounter large osmotic gradients in an intact animal.

In Hap1 and HeLa cells, the large cytoplasmic vacuoles observed under hypotonic stress contained markers for late endosomes and lysosomes, including lysosomal associated membrane protein 1 (LAMP1) (*SI Appendix*, Fig. S1 *A* and *B*), Rab7 (*SI Appendix*, Fig. S1*C*), Dextran-Green (an endocytic marker that reaches lysosomes at steady state) (*SI Appendix*, Fig. S1*D*), or LysoTracker (a lysosomal pH indicator) (*SI Appendix*, Fig. S1*D*) (20, 21). In contrast, most insult-induced vacuoles were not immunopositive for an early endosomal marker (EEA1) (*SI Appendix*, Fig. S1*E*), nor for markers of endoplasmic reticulum (ER) or mitochondria, suggesting that late endosomes and lysosomes (referred to as lysosomes for simplicity hereafter) are likely the primary vacuolar membrane source.

A super resolution fluorescence imaging assay was used to quantify the volume of lysosomes and vacuoles in both Hap1 cells and HeLa cells as a function of osmotic strength (Fig. 1*B*, *SI Appendix*, Fig. S1*F*, and Movie S1). The principle of the assay is that Dextran-Green is trapped in the lumen of lysosomes and endosomes (22, 23), and LAMP1-mCherry fluorescence allows one to identify lysosomes (20) so, for each green object surrounded by red fluorescence, the length of the green region (or the distance between the two peaks of red fluorescence that surround it) is the diameter of the object. Thus, we can estimate lysosomal volume by treating each object as a sphere with Volume $=\frac{4}{3}*\text{pi}*\left(\frac{Distance}{2}\right)^3$. At 300 mOsm, the diameter of all lysosomes was small, but, as the osmolarity was decreased from the control level to 220 or 170 mOsm, the diameter of some lysosomes enlarged to over 2 μm while others remained much smaller (Fig. 1*B* and *SI Appendix*, Fig. S1*F*). As compared to 300 mOsm solution (mean volume 0.006 ± 0.003 μm^3), the average volume of lysosomes increased about fivefold at 220 mOsm (0.031 ± 0.011 μm^3) and more than 100-fold at 170 mOsm (0.705 ± 0.135 μm^3) (*SI Appendix*, Fig. S1*G*). In contrast, early endosomes were not enlarged by exposure to the 170-mOsm solution (*SI Appendix*, Fig. S1*H*). Large vacuoles without green dextran labeling were occasionally observed (one example is present on the left side of the cell at 170 mOsm illustrated in Fig. 1*B*), but these represented only 4.7% of all vacuoles. These vacuoles without green fluorescence appeared to have a rim of LAMP1 staining, but, without the Dextran-Green labeling to cleanly define that the LAMP1 was on the vacuole membrane, we could not confirm that they were of lysosomal origin. Nevertheless, we conclude that at least 95% and probably all giant cytoplasmic vacuoles of mammalian cells observed following hypoosmotic challenge are enlarged lysosomes.

Lysosome-Derived Vacuoles Express Chloride Channels Gated by Low Ionic Strength. The plasma membranes of many mammalian cell types express ion channels that respond to changes in the osmotic strength of the bathing medium. We used whole-endolysosome (whole-EL) patch-clamp recording (Fig. 1*C* and *SI Appendix*, Fig. S2*A*) to test whether osmolarity-sensitive ion channels were present on vacuolated lysosome membranes. Vacuoles were produced by exposing Cos1 cells to 80 mOsm solution. Whole-EL recordings were then established in the same solution, and the current–voltage relation was determined by the responses to voltage ramps from -120 mV to +120 mV. Large outwardly rectifying currents were observed at positive membrane potentials and were greatly decreased by transferring to 320 mOsm, or exposure to DCPIB, a small molecule usually used as a pharmacological tool for ion channel studies, including VRAC (24, 25) (Fig. 1*D*). Responses to voltage steps showed there was relatively little voltage-dependent activation or deactivation to the currents present in the 80-mOsm solution (Fig. 1*E*). Because the activation mechanism of the plasma membrane osmotic-sensitive channel VRAC is controversial, with both cytosolic low ionic strength (14, 17, 26) and extracellular hypotonicity (15, 16) suggested to be the relevant signal, we tested solutions of a variety of osmolarities and ionic strengths (Γ) in both the intracellular/cytosolic/bath and luminal/pipette solutions. We concluded that reduced intracellular ionic strength (Γ_i) is likely to be the primary stimulus causing dose-dependent activation of current (*SI Appendix*, Fig. S2*B* and *Supplemental Discussion*). Recordings from vacuoles enlarged by chemical treatment with vacuolin-1 (27) (Fig. 1 *F* and *G*) or by overexpression of TMEM106B-GFP (28) (*SI Appendix*, Fig. S2*C*) also showed outwardly rectifying currents that were very small at Γ_i 140 and greatly increased at Γ_i 40. Following a change in cytosolic ionic strength, it required several minutes until the currents induced by the change reached their peak amplitude (Fig. 1*F*), which was dependent on the cytosolic ionic strength (Fig. 1*H*).

With our standard recording solutions, the ionic strength-sensitive current of the lysosome had a reversal potential (E_{rev}) of −31.8 ± 1.6 mV (Fig. 1*I* and *SI Appendix*, Fig. S2*C*), close to the equilibrium potential for Cl^- (calculated E_{rev} = −32.2 mV based on $[Cl^-]_{Lumen}$ = 140 mM and $[Cl^-]_{Cytosol}$ = 40 mM). Removal of Na^+ or K^+ from the luminal/pipette or cytosolic/bath solution did not affect the ionic strength-sensitive current (*SI Appendix*, Fig. S2*D*) nor did changing the pH between 4.6 and 7.2 (*SI Appendix*, Fig. S2*E*) whereas changing $[Cl^-]_{Lumen}$ resulted in Nernstian shifts in E_{rev} (Fig. 1*I*). Other anions, including NO_3^-, HCO_3^-, acetate$^-$, aspartate$^-$, and glutamate$^-$ were also permeable (P_X/P_{Cl} = 0.2~2) (*SI Appendix*, Fig. S2*F*). We therefore refer to the channel carrying this current as the Lyso-VRAC. Three compounds known to inhibit PM-VRACs (DCPIB, CBX, and R(+)-IAA94) (25, 29) also inhibited Lyso-VRACs (Fig. 1*D* and *SI Appendix*, Fig. S3).

Lyso-VRAC currents were present in vacuoles from all cell types that we investigated, including Cos1, Hap1, Hap1–KI GFP, HEK293T, human breast cancer cells (MDA231), primary mouse embryonic fibroblasts (MEFs), and bone marrow macrophages (BMMs) (Fig. 1*J*). In sharp contrast, when recordings were made from enlarged early endosome membranes, no Lyso-VRAC–like current was detected (*SI Appendix*, Fig. S2*G*).

The Lyso-VRAC Current Is Mediated by LRRC8 Proteins. LRRC8A codes for an essential subunit of the PM-VRAC. Because of the great similarity between the electrophysiological and pharmacological properties of Lyso-VRAC and PM-VRAC, we tested whether LRRC8A is also an essential subunit of Lyso-VRAC by

making *LRRC8A* knockout (*8A* KO) cell lines in both Hap1 and HeLa cells using the CRISPR-Cas9 system (30) (*SI Appendix*, Fig. S4 *A* and *B*). Γ_i 40 solutions failed to induce any current in *8A* KO Hap1 cells (Fig. 2*A*), *8A* KO HeLa cells (*SI Appendix*, Fig. S4 *C* and *E*), or in bone marrow cells from *ebo*/*ebo* mice (*SI Appendix*, Fig. S4 *D* and *E*), which have a frameshift mutation (31) in exon 3 of the LRRC8A gene. PM-VRAC current was rescued by 8A-mCherry transfection (*SI Appendix*, Fig. S2*F*), but Lyso-VRAC was not (*SI Appendix*, Fig. S4*G*). Lyso-VRAC is highly permeable to aspartate$^-$ (*SI Appendix*, Fig. S2*F*), a property that requires either LRRC8D or -E in PM-VRAC (29, 32), and so we tested if these subunits contribute to Lyso-VRAC currents. Lyso-VRAC currents were restored in *8A* KO Hap1 cells by coexpression of 8A-mCherry and 8E-GFP (Fig. 2 *B* and *C* and *SI Appendix*, Fig. S4*H*) or 8A-mCherry and 8D-GFP (*SI Appendix*, Fig. S4*I*). To keep the total number of experiments manageable, we focused all remaining experiments on the 8A plus 8E combination.

To determine the intracellular localization of LRRC8 family proteins, we examined the location of LRRC8A and LRRC8E using Western blots of proteins isolated from cell fractions enriched in lysosomes and imaging of fluorescent fusion proteins. To explore the localization of LRRC8A at normal expression levels, we made knock-in Hap1 cells (GFP-KI) so that expression of the fusion protein was controlled by the endogenous LRRC8A promoter. Western blot analysis of lysosomes isolated by gradient-based centrifugation or immunoisolation (33) demonstrated that these organelles were enriched for endogenous (Fig. 2*D*) and overexpressed LRRC8A proteins (*SI Appendix*, Fig. S5*A*).

When LRRC8A-GFP knock-in cells were exposed to solutions of normal osmotic strength (300 mOsm), there was fluorescence on the plasma membrane and brighter fluorescence localized to intracellular puncta which primarily colocalized with LAMP1 (Fig. 2*E*) and barely any colocalization with early endosome markers (*SI Appendix*, Fig. S5*B*). Thus intracellular LRRC8A is associated mainly with lysosomes. In cells transiently transfected

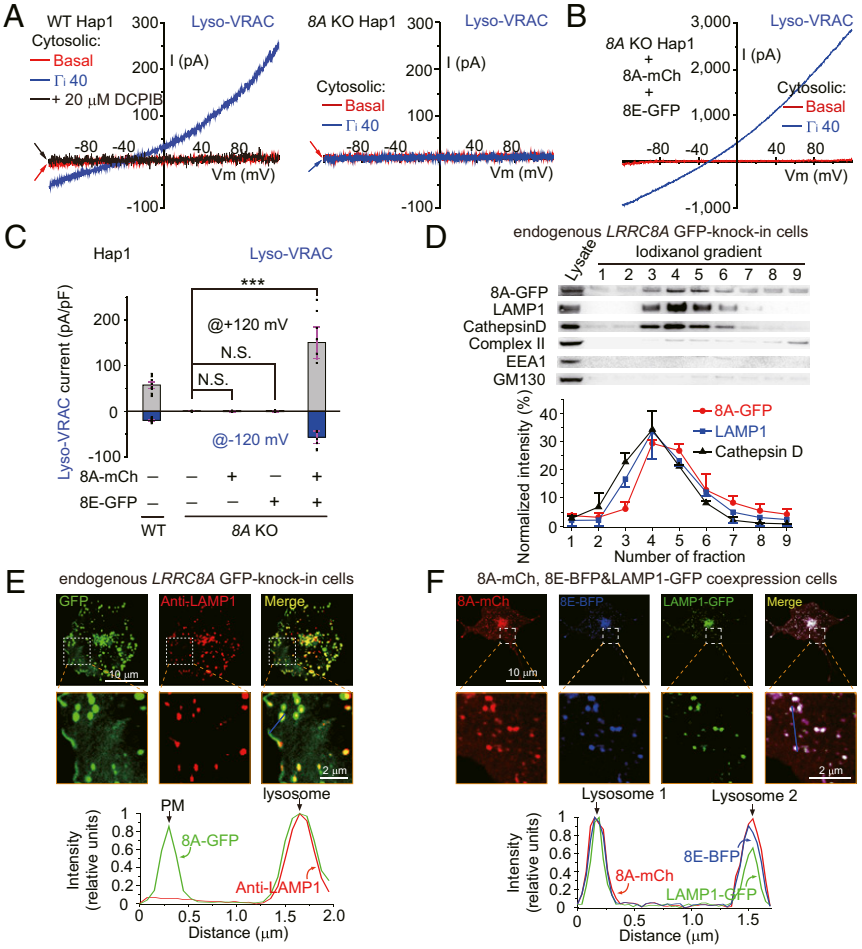

Fig. 2. LRRC8 proteins are required to produce Lyso-VRAC. (*A*) $I_{Lyso\text{-}VRAC}$ from endolysosomes enlarged with vacuolin-1 in WT and *8A* KO Hap1 cells with basal and low ionic strength bath solutions. $[Cl^-]_{Pipette/Lumen}$ = 140mM, and $[Cl^-]$ = 40mM for Γ_i 40. DCPIB was applied in the Γ_i 40 solution. (*B*) $I_{Lyso\text{-}VRAC}$ in *8A* KO Hap1 cells dually transfected with LRRC8A-mCherry and LRRC8E-GFP. (*C*) Current density of $I_{Lyso\text{-}VRAC}$ in WT and in *8A* KO Hap1 with or without overexpressed LRRC8 proteins. Current densities at ±120 mV are shown. Data for each condition were assessed for significance using Student`s *t* test and were collected from six or more independent experiments. *** is $P < 0.001$ and "N.S." is $P > 0.05$. (*D*) Subcellular fractionation analysis of LRRC8A-GFP expression in various organelle fractions of LRRC8A-GFP–knock-in Hap1 cells. The organelle-specific markers identified in these Western blots were as follows: Lysosomes, LAMP1 and Cathepsin D; Mitochondria, Complex II; Early Endosomes, EEA1; and the Golgi apparatus, GM130. Similar data were collected from three independent experiments, and the graph shows the means ± SEMs. (*E*) The expression pattern of LRRC8A-GFP when this coding sequence was knocked into the endogenous location of *LRRC8A* in Hap1 cells. Lysosomes were labeled by immunostaining for LAMP1 (red). The boxed regions in the *Upper* images are shown at higher magnification in the *Lower* images. The graph below each group of images is a line scan through the plasma membrane and lysosome shown in the boxed region indicating the intensity of 8A-GFP (green lines) and Anti-LAMP1 (red lines) along the blue line. (*F*) Images and line scan analysis showing the colocalization of 8A-mCherry (red), 8E-BFP (blue), and LAMP1-GFP (green) in transfected Cos1 cells.

so that a fusion protein of LRRC8A-mCherry was expressed at high levels, imaging demonstrated abundant labeling on both the plasma membrane and on lysosomal membranes (*SI Appendix*, Fig. S5*C*). When wild-type (WT) LRRC8E fused to a fluorescent protein was overexpressed, very little fluorescence was localized to the lysosome (*SI Appendix*, Fig. S5*D*), with most fluorescence localized to the ER (*SI Appendix*, Fig. S5*E*). However, when both LRRC8A and LRRC8E fusion proteins were coexpressed at high levels, intracellular LRRC8E as well as intracellular LRRC8A localized mostly to lysosomes (Fig. 2*F*). In these experiments, the colocalization of the two LRRC8 proteins was extensive. Unlike membrane proteins targeted to lysosomes for degradation, which are expected to be localized to intraluminal vesicles (20), after hypotonic challenge, almost all of the intracellular LRRC8A and LRRC8E signal was localized to the perimeter membranes of the lysosome-derived large vacuoles (*SI Appendix*, Fig. S5*F*). Thus, the distribution of LRRC8 proteins on vacuoles is consistent with the large Lyso-VRAC currents recorded from vacuole membranes.

Lyso-VRAC Requires a Double-Leucine Motif of LRRC8A. Like many lysosomal membrane proteins that use an AP-2–dependent internalization route for lysosomal targeting (20), LRRC8A contains two double-leucine (LL) motifs near the intracellular C terminus. Mislocalization of other lysosomal membrane proteins with their LL domains deleted is known to be due to impaired internalization and also a secondary block of anterograde trafficking (34). Mutation of the $L^{706}L^{707}$ motif to alanines (Fig. 3*A*) was sufficient to abolish lysosomal localization of transfected LRRC8A, and the mutant protein was instead found on the plasma membrane and in the ER (*SI Appendix*, Fig. S5*G*). However, unlike coexpression with wild-type subunits, high level coexpression of $8A^{L706A,L707A}$-mCh and wild-type LRRC8E-GFP gave very little lysosomal expression of either (Fig. 3*B*). Although the subunit stoichiometry of Lyso-VRAC in native lysosomes is not yet known, these results suggest that LRRC8A is required for other LRRC8 proteins to reach lysosomes.

Consistent with the imaging data, cotransfection of $8A^{L706A,\ L707A}$-mCherry and 8E-GFP failed to produce Lyso-VRAC in *8A* KO

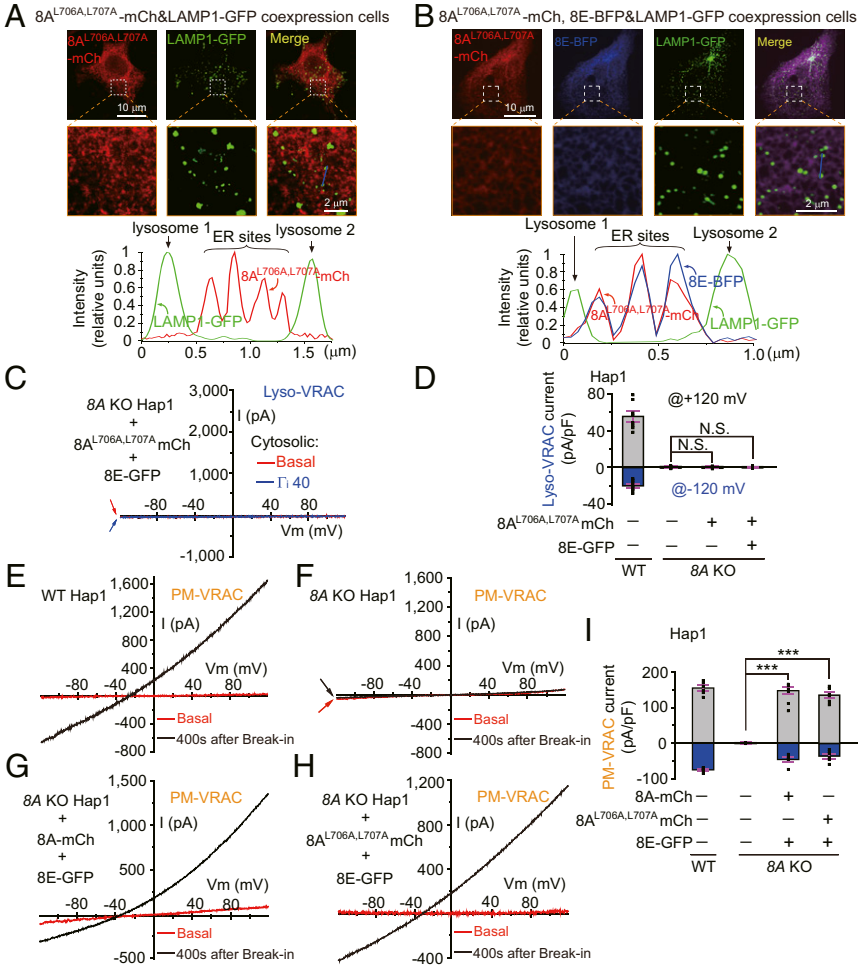

Fig. 3. A double-Leucine motif is required for lysosomal localization of LRRC8A to mediate Lyso-VRAC. (*A*) Images and line scan analysis showing the lack of colocalization of $8A^{L706A,L707A}$-mCherry (red) and LAMP1-GFP (green) in transfected Cos1 cells. See *SI Appendix*, Fig. S5*G* for evidence that the $8A^{L706A,L707A}$-mCherry staining is in the ER. (*B*) Images and line scan analysis showing that $8A^{L706A,L707A}$-mCherry (red) and 8E-BFP (blue) localized to a different organelle than LAMP1-GFP (green) in transfected Cos1 cells. (*C*) Representative traces of $I_{Lyso\text{-}VRAC}$ in *8A* KO Hap1 cells dually transfected with $8A^{L706A,L707A}$-mCherry and 8E-GFP. (*D*) Current density of $I_{Lyso\text{-}VRAC}$ in WT and in *8A* KO Hap1 with or without overexpressed $8A^{L706A,L707A}$-mCherry and 8E-GFP. Data for each condition in this panel and in *I* were assessed for significance using Student`s *t* test and were collected from six or more independent experiments. (*E* and *F*) Whole cell recordings to test for plasma membrane VRAC (PM-VRAC) currents in WT and *8A* KO Hap1 cells. These experiments used Γ_i 40 ($[Cl^-]$ = 40 mM) as the cytosolic/pipette solution and Γ_i 140 ($[Cl^-]$ = 140 mM) as the extracellular/bath solution. The responses are shown at 0 (red) and 400 s (black) after break-in. (*G*) Experiment similar to *E* except that the *8A* KO Hap1 cells were cotransfected with 8A-mCherry and 8E-GFP. (*H*) Experiment similar to *E* except that the *8A* KO Hap1 cells were transfected with $8A^{L706A,L707A}$-mCherry and 8E-GFP. (*I*) Current density of $I_{PM\text{-}VRAC}$ in WT and *8A* KO Hap1 cells with or without LRRC8 proteins overexpressed. *** is $P < 0.001$ and "N.S." is $P > 0.05$.

Hap1 cells (Fig. 3 *C* and *D*). Therefore, lysosome-targeted LRRC8A and at least one of the other LRRC8 proteins are required for the Lyso-VRAC current. However, the PM-VRAC current was fully restored in *8A* KO Hap1 cells by coexpression of 8E-GFP together with either LRRC8A or $8A^{L706A,\ L707A}$-mCherry (Fig. 3 *E–I*). Hence, there are distinct trafficking mechanisms that regulate the expression of Lyso-VRAC versus PM-VRAC, suggesting that the biological roles of Lyso-VRAC and PM-VRAC can be distinguished. In summary, *8A* KO cells coexpressing $8A^{L706A,\ L707A}$-mCherry and 8E-GFP are essentially PM-VRAC (+) but Lyso-VRAC (−) cells.

Lyso-VRAC Plays a Critical Role in Lysosome Vacuolation. *8A* KO Hap1 and HeLa cells did not become vacuolated under hypoosmotic challenge (Fig. 4*A*), nor did BMM cells from *ebo/ebo* mice (*SI Appendix*, Fig. S6*A*), but lysosomal vacuolation remained normal when several other lysosomal channels were knocked out (Fig. 4*A*). It should be noted that *8A* KO cells swell dramatically when given a hypotonic challenge, and, when they are adherent and tightly packed, most of their expansion is up from the surface of the dish (Movie S2). However, the *8A* KO did not prevent lysosomal vacuolation caused by vacuolin-1 (27) or the vacuolating cytotoxin VacA (35) (*SI Appendix*, Fig. S6*B*).

The ability to selectively rescue VRAC expression in *8A* KO cells only on the plasma membrane (by coexpressing $8A^{L706A,\ L707A}$ and 8E) or on the plasma membrane and in lysosomes (by coexpressing WT 8A and 8E) allowed us to test the relative biological importance of PM-VRAC and Lyso-VRAC. In response to a hypotonic challenge, cells expressing VRAC only on the plasma membrane were incapable of expanding the volume of their lysosomes (Fig. 4*B*) and incapable of forming giant vacuoles (Fig. 4*C*). In contrast, expressing VRAC on both the plasma membrane and lysosome membranes completely restored the ability to expand the volume of lysosomes and nearly completely restored the ability to form giant vacuoles.

DCPIB at 20 μM completely blocked both Lyso-VRAC and PM-VRAC current (*SI Appendix*, Fig. S6 *C* and *F*). In DCPIB-treated WT cells, no lysosomal volume increase or vacuolation in response to hypoosmotic challenge was observed (Fig. 4 *D* and *E*). Thus, channel function of VRAC somewhere in the cell is essential for lysosome vacuolation under hypoosmotic challenge. The critical location was revealed by use of the VRAC inhibitor NS3728, which is negatively charged (36) and membrane impermeable (37). NS3728 completely inhibited PM-VRAC (studied with whole-cell recording) at all membrane potentials when present at 10 μM in the extracellular solution and absent from the pipette solution (*SI Appendix*, Fig. S6 *D* and *F*). However, when the same concentration of NS3728 was present in the solution bathing the exposed cytosolic face of vacuoles (studied with whole lysosome recording), there was no detectable inhibition of Lyso-VRAC at negative membrane potentials and <10% inhibition at the most positive potential studied (*SI Appendix*, Fig. S6 *E* and *F*). A likely reason for the failure of NS3728 to inhibit Lyso-VRAC but potently inhibit PM-VRAC is that the NS3728 binding site is on the luminal surface, which is facing extracellular for PM-VRAC (37), but hidden behind two membranes for Lyso-VRAC (*Discussion*). NS3728 was therefore a powerful pharmacological tool to create PM-VRAC (−) but Lyso-VRAC (+) cells for further dissection of the role of Lyso-VRAC in lysosome vacuolation. In Hap1 cells treated with NS3728 (30 μM for 2 h), lysosome vacuolation was not diminished (Fig. 4*D*) so PM-VRAC, which is blocked by NS3728 is not required for this process. We infer that DCPIB must be blocking vacuolation by acting on Lyso-VRAC so activation of Lyso-VRAC is necessary for lysosome vacuolation under hypoosmotic stress.

We also identified an additional manipulation that prevented vacuolation to hypotonic stress. A key feature of lysosomal physiology is the highly acidic lumen (20), which is required for many lysosome functions and is produced by the activity of a V-ATPase that can be inhibited by Bafilomycin A1 (Baf-A1) (38). When Baf-A1was present, prolonged treatment with a 170-mOsm solution produced no vacuolation in either Hap1 or HeLa cells (*SI Appendix*, Fig. S7).

Lysosomes Maintain Intracellular Water Homeostasis. Under hypoosmotic challenge, H_2O influx mediated by aquaporins on the plasma membrane has been reported to reduce the osmolarity and ionic strength of the cytosol (39). Exposure to 50 μM Hg^{2+}, which blocks aquaporin activity, eliminated hypotonicity-induced volume increases (*SI Appendix*, Fig. S8*A*) and lysosomal vacuolation in Hap1 cells (Fig. 5*A*). Therefore low expression or activity of aquaporin on a subset of cells might explain why some cells failed to become vacuolated in response to hypotonicity over the time course of our other experiments. Furthermore, high expression of aquaporin should rapidly bring the intracellular ionic strength into the range that we showed activates Lyso-VRAC. A fluorescence assay was used to investigate water flow across the lysosomal membrane. Lysosomes within intact cells were loaded with Lucifer yellow dextran (LY-Dextran), which displays enhanced fluorescence in the presence of deuterated water (D_2O) (40). Hypoosmotic challenge with D_2O quickly augmented the fluorescence intensity (Fig. 5*B* and Movie S3), indicating that there is substantial water flux into the lumen of lysosomes from the cytosol soon after water penetration across the plasma membrane. Time-lapse video observations of vacuolin-1 enlarged lysosomes released from cells by microdissection demonstrated that, within a few minutes of exposure to 170 mOsm solution, they "swell," "blur," and eventually have their membranes rupture (*SI Appendix*, Fig. S8*B*). Measurement of alkaline phosphatase released into the medium from purified lysosomes suggests that, under cell-free conditions, Lyso-VRAC enhances lysosome lysis since the amount of activity released was substantially decreased when lysosomes from WT cells were treated with DCPIB or the lysosomes came from *8A* KO cells (*SI Appendix*, Fig. S8*C*). Selective sequestration of intracellular water into vacuolated lysosomes would not reduce cytoplasm volume (the total volume enclosed by the plasma membrane) but would effectively reduce cytosol volume (the parts of the cytoplasm that are not enclosed by organelle membranes) and so help restore the optimal physiological concentrations of proteins and metabolites and contribute to maintaining the health of the cell (*SI Appendix*, Fig. S8*D*).

As a consequence of the water influx across the plasma membrane during hypotonic challenge, cell volume initially increases dramatically (Fig. 5 *C–E*). Based on published calibration curves for the assay we used (42, 43), the increase to 125% of the basal fluorescence at the peak of the response indicates that the cell volume increased nearly threefold and so presumably dropped the intracellular ionic strength from Γ140 to about one-third its normal level, which can activate substantial Lyso-VRAC current (Fig. 1*H*). In WT HeLa and Hap1 cells, volume begins to return toward normal after about 15 to 20 min. This regulatory volume decrease (RVD) was prevented in WT cells by DCPIB (Fig. 5*C*), which blocks both PM-VRAC and Lyso-VRAC, and was absent in HeLa and Hap1 *8A* KO cells that lack both PM-VRAC and Lyso-VRAC (Fig. 5 *C–E*). RVD was largely restored in 8A KO cells by coexpressing LRRC8A and LRRC8E, which rescues both PM-VRAC and Lyso-VRAC (Fig. 5*D*). A treatment that rescued only PM-VRAC in *8A* KO cells (the combination of $8A^{L706A,\ L707A}$ and 8E) did not restore RVD (Fig. 5*D*), indicating that vacuolar LRRC8 proteins are necessary for RVD (*SI Appendix*, Fig. S8*D*). Conversely, NS3728 treatment, which blocks only PM-VRAC, also prevented RVD (Fig. 5*E*), indicating that plasma membrane LRRC8s are also necessary for RVD. Taken together, these experiments thus demonstrate a dual requirement for both PM-VRAC and Lyso-VRAC.

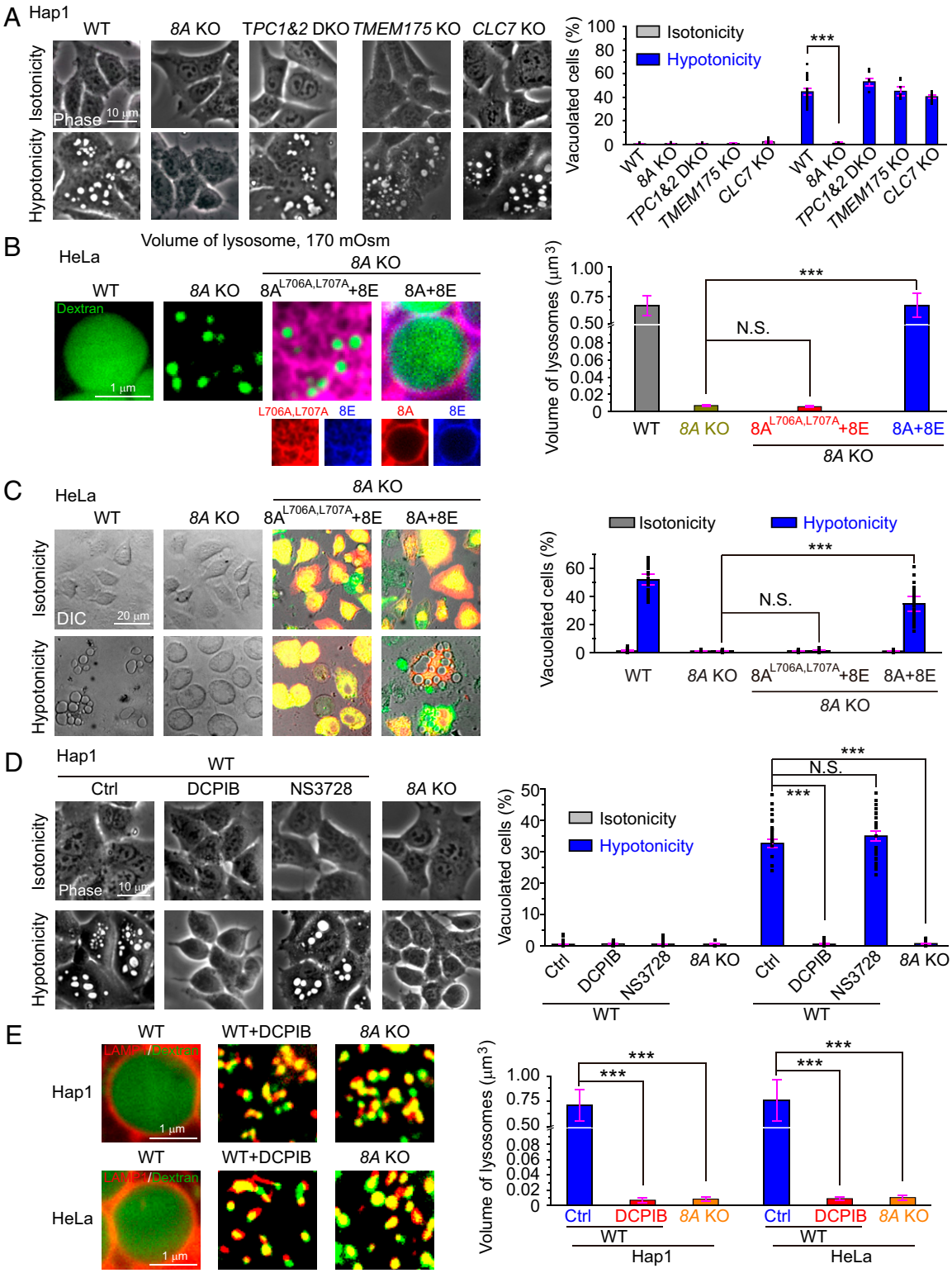

Fig. 4. Lyso-VRAC is required for hypotonicity-induced lysosomal vacuolation. (*A*) Hypotonicity-induced cytoplasmic vacuolation in WT, *8A* KO, *TPC1&2* double KO (DKO), *TMEM175* KO, and *CLC7* KO Hap1 cells. Quantitative analysis is to the *Right*. In all panels with asterisks *** is $P < 0.001$ and N.S. is $P > 0.05$. (*B* and *C*) Sample images (*Left*) and quantitative analysis (*Right*) of lysosomal volume expansion (*B*) and lysosome vacuolation (*C*) under hypotonic stress in *8A* KO HeLa cells that were dually transfected with 8E-BFP + 8A-mCherry or $8A^{L706A,L707A}$-mCherry. (*D*) Differential effects of NS3728 (30 μM; membrane-impermeable) and DCPIB (100 μM, membrane-permeable) VRAC inhibitors on hypotonicity-induced vacuolation in WT and *8A* KO Hap1 cells. (*E*) Effect of 100 μM DCPIB and LRRC8A knock out on lysosomal volume. In all bar graphs, data points were collected from more than six independent experiments, and Student`s *t* test was used to determine significance.

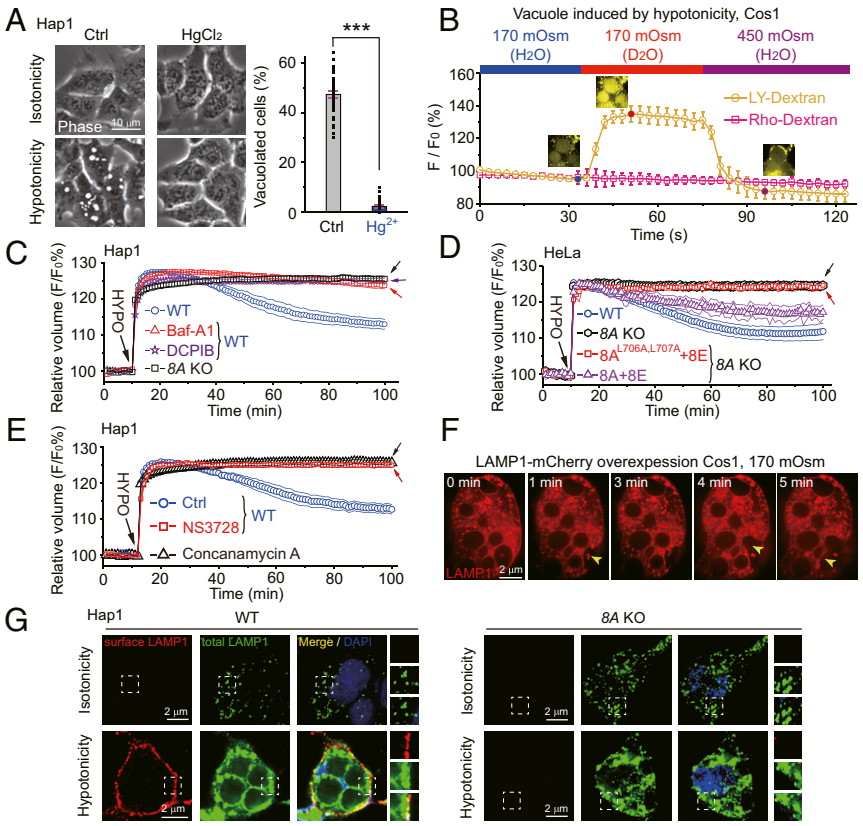

Fig. 5. Lysosomes store and expel intracellular water to regulate cytosolic RVD. (*A*) Representative images (*Left*) and quantitation (*Right*) of effects of 50 μM $HgCl_2$ (an aquaporin inhibitor) on lysosome vacuolation induced by hypotonicity. *** is $P < 0.001$. (*B*) Fluorescence of Lucifer yellow dextran (LY-Dx, yellow) and Rhodamine dextran (Rho-Dx, red) in response to D_2O- or H_2O-containing hypotonic (170 mOsm) solutions in Cos1 cells. Also see Movie S3. LY-Dextran and Rho-Dextran were preloaded into lysosomes of Cos1 cells by endocytosis. (*C–E*) Time course of regulatory cytosol volume decrease (RVD) in response to 110-mOsm solutions estimated by measuring the fluorescence intensity of Calcein-AM (41). The concentrations of drugs used were 5 μM Baf-A1, 100 μM DCPIB, 30 μM NS3728, and 20 μM Concanamycin A. (*F*) Snapshots of a Cos1 cell transfected with LAMP1-mCherry from a time-lapse series. Time 0 is defined as 78 min after the onset of the cell being placed in 170 mOsm medium to induce production of large vacuoles (also see Movie S4). Exocytosis events are indicated with yellow arrowheads at 1, 4, and 5 min. (*G*) Effects of hypotonic treatment (0.5 h) on LAMP1 surface staining in WT (*Left*) and *8A* KO (*Right*) Hap1 cells. Cells were immunostained using an anti-LAMP1 antibody that recognized an extracellular/luminal epitope under conditions that first stained only plasma membrane LAMP1 (nonpermeabilized cells, red) and then total LAMP1 (permeabilized cells, green). Nuclei were counterstained with DAPI (blue). Zoomed-in images of the boxed regions are shown in *Right*. In *B–E*, data points were collected from six independent experiments.

RVD could also be suppressed in WT cells by two V-ATPase inhibitors (Baf-A1 and Concanamycin A) (Fig. 5 *C* and *E*). Chemically induced lysosome vacuolation by vacuolin-1 did not restore RVD in *8A* KO cells, even when PM-VRAC activity was restored by expressing $8A^{L706A,L707A}$ (*SI Appendix*, Fig. S8 *E* and *F*).

Water entering lysosomes and enlarging them into vacuoles might help restore the normal ionic strength and osmolarity of the cytosol but would not relieve the plasma membrane tension stress. Previous studies had demonstrated that intracellular membrane exocytosis occurs in response to hypoosmotic stress (8, 9). By making time-lapse video observations of Cos1 cells expressing fluorescent LAMP1, we demonstrated that lysosome-derived giant vacuoles underwent exocytosis (Fig. 5*F* and Movie S4). Another consequence of lysosome exocytosis was a greatly increased abundance of LAMP1 on the plasma membrane (Fig. 5*G*). Thus, just as the mammalian bladder fills with wastes from the kidney and then discharges the waste and any excess water to the outside of the animal, lysosomes serve as the cell`s "bladder," sequestering intracellular excess water through vacuolation and then expelling the potentially toxic level of water through exocytosis, which also relieves the plasma membrane tension stress.

Lyso-VRACs Protect Cells from Necrotic Cell Death in Response to Multiple Types of Physiological Stress. Vacuolization followed by exocytosis and RVD occurs within an hour of exposure to hypotonic stress. However, when cells encounter a sustained stress, substantial necrotic cell death resulted, whether assessed by propidium iodide (PI) staining or by lactate dehydrogenase (LDH) release into the medium. The imaging-based assay (Fig. 6*A*) also showed that becoming vacuolated is highly correlated with survival. Under the tested conditions (80 mOsm solution for 1 h), only 0.4% of the cells that were vacuolated died (i.e., became PI positive), but 46.9% of the non-vacuolated cells died (N> 600 randomly selected cells from six independent experiments). Lyso-VRAC plays an important role in survival under these conditions because the survival index calculated from LDH activity release was much lower in LRRC8A KO cells, and survival was restored to close to WT levels when *8A* KO cells were cotransfected with 8A plus 8E, but not with $8A^{L706A,L707A}$ plus 8E (Fig. 6*B*).

We also tested the importance of Lyso-VRAC for successful responses to two other stresses capable of causing necrotic cell death: hypoxia and hypothermia. As was the case for hypotonic stress, the propidium iodide assay showed that the survival of nonvacuolated cells in response to these stresses (29.1% death

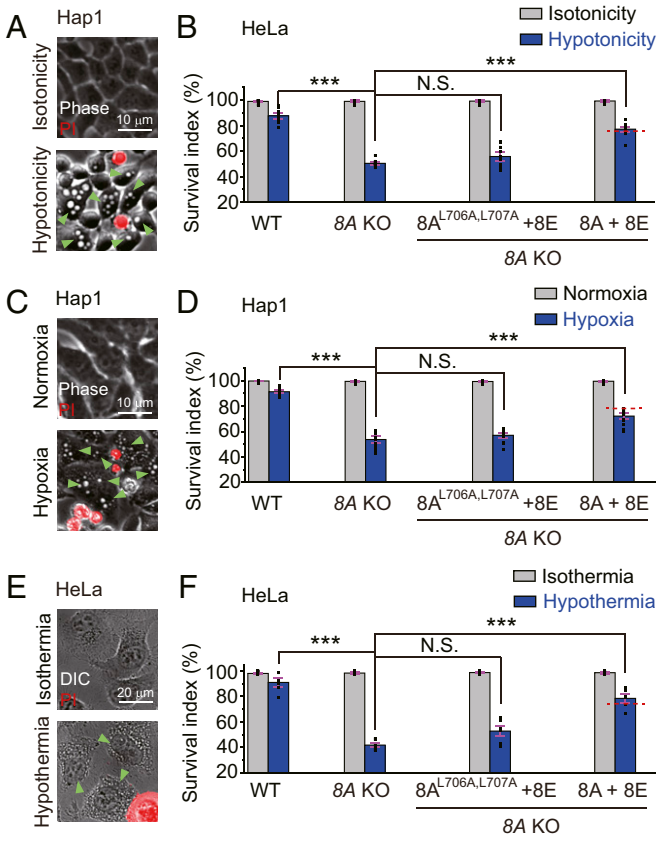

Fig. 6. Lyso-VRAC protects cells from necrotic death to multiple stressors. Effects of 1 h hour of treatment with hypotonicity (80 mOsm; *A* and *B*), hypoxia (5% O_2; *C* and *D*), and hypothermia (4 °C; *E* and *F*) on cell survival of Hap1 or HeLa cells. In all panels with asterisks *** is $P < 0.001$ and N.S. is $P > 0.05$. (*A*, *C*, and *E*) Representative images of cells stained with propidium iodide (red) to identify necrotic cells, viewed with phase contest microscopy. Cells with vacuoles are indicated with green arrowheads. (*B*, *D*, and *F*) Cell survival assayed by measuring extracellular LDH activity for samples from the indicated cell type. LDH activity for each group of cells was normalized as the percentage of the LDH activity released from the same number of cells by treatment with distilled water (which caused all cells to die). The survival index was then calculated as 100%-relative LDH activity.

for hypoxic stress and 38.6% death for hypothermic stress) was much worse than the survival (<0.5% death) of cells that had vacuoles visible (Fig. 6 *C* and *E*) (more than 600 cells were examined from six independent experiments.). Cotransfection of LRRC8A KO cells with LRRC8E plus LRRC8A resulted in significantly more survival than cotransfection with LRRC8E plus $8A^{L706A,L707A}$ for both stresses so Lyso-VRAC enhances survival to these stresses as well (Fig. 6 *D* and *F*). However, NS3728, which does not inhibit Lyso-VRAC but does inhibit PM-VRAC, results in a level of cell death to 80 mOsm solution similar to the amount observed in the LRRC8A KO (*SI Appendix*, Fig. S9*A*) so VRACs are needed at both locations to stave off cell death to this intensity of hypoosmotic stress.

Acute treatment with 5 μM Baf-A1 prevented vacuolation in response to hypoosmotic stress, but prolonged treatment with Baf-A1 had no effect on Hap1 cell survival when these cells were maintained under control osmotic conditions (*SI Appendix*, Fig. S9 *B–F*). However, Baf-A1 greatly increased the extent of necrotic cell death caused by hypoosmotic stress (*SI Appendix*, Fig. S9 *B–D*), hypoxic stress (*SI Appendix*, Fig. S9*E*), or hypothermic stress (*SI Appendix*, Fig. S9*F*). A final feature shared by necrotic cell death induced by hypotonicity, hypoxia, and hypothermia is that all required functional synaptotagmin-VII to protect against the stress. The evidence for this conclusion is that transfection with a dominant negative Synt-VII construct, which has no effect on the survival of cells under normal conditions, leads to cell death as severe as the *8A* knockout when cells are subjected to each of these stresses (*SI Appendix*, Fig. S10 *A–C*). This requirement for Synt-VII is likely because it is required for lysosome exocytosis (20).

Discussion

In an intact animal, the bladder stores and expels urine. We provide compelling evidence that, in individual cells, lysosomes play a critical role in alleviating the intracellular water crisis caused by hypotonic stress by acting as the cell`s "bladder." Lysosomes sequester water, an action that will help to restore the optimal physiological concentrations of proteins and metabolites. Lysosome-derived vacuoles then fuse with the plasma membrane, an action that by expelling water helps restore the cell volume to its original size. According to the "square-cube law," volume increases in proportion to the cube of the diameter, but surface area only increases in proportion to the square of the diameter. Thus, by placing the amount of membrane surface area that is present in a very large number of lysosomes into a much smaller number of large vacuoles, a huge increase in luminal volume becomes available for water storage. Lysosomal exocytosis also delivers more materials to the plasma membrane, both lipids and lysosome resident proteins. This will substantially relieve membrane tension stress and allow larger PM-VRAC currents than the channels originally located there could produce (Fig. 7).

We demonstrated that Lyso-VRAC, but not PM-VRAC, is essential for lysosomal vacuolation, but both are required to ultimately allow the cell to survive. However, other stressors also produce vacuoles, and cell survival is much greater with functional Lyso-VRAC so its role may not be limited to cellular osmoregulation. It is not yet clear why VRACs at two locations are necessary for successful RVD and cell survival, but one appealing idea is that the processes they regulate are in series so, if either fails, osmoregulation fails. Testing this idea requires the ability to have temporal control over when each VRAC is active, but at present this is only possible for PM-VRAC.

As far as the relationship between the opening of Lyso-VRACs, lysosomal swelling, and vacuolation, it seems unlikely that chloride flowing down its electrochemical gradient is the direct cause because estimates of the lysosome membrane potential and chloride gradient (21, 44–46) suggest that, when Lyso-VRAC channels open, chloride flows from the lysosome into the cytosol, which would lessen the osmotic force driving water into the lysosome, not increase it. One factor that could play a role is that Lyso-VRAC channels are permeable to multiple organic anions (*SI Appendix*, Fig. S2*F*) so one that is normally absent from lysosomes but present in the cytosol could enter the lysosome when Lyso-VRACs open, drawing some water after it. However, once this anion's concentration equilibrated with the cytosol concentration, water movement due to this effect would cease so, to produce enough water movement to produce substantial osmotic swelling, the normal concentration of this ion in the cytosol would have to be very high. Therefore, another possibility needs to be considered. VRACs are suspected to be directly permeable to water as well as anions (47). Perhaps, in the basal state, the water permeability of lysosomes is very low (moving only through the lipid bilayer), and the majority of osmotically active lysosome constituents are metabolic breakdown products that are also membrane impermeable. In this scenario, under hypoosmotic conditions, as water flows across the plasma membrane, the cytosol begins to dilute as the cell volume increases, but, for a while, lysosome volume is unchanged because rapid water flux is not possible. When the cytosol ionic strength has fallen sufficiently to open Lyso-VRAC channels, water can rapidly flow into the lysosome, but most of

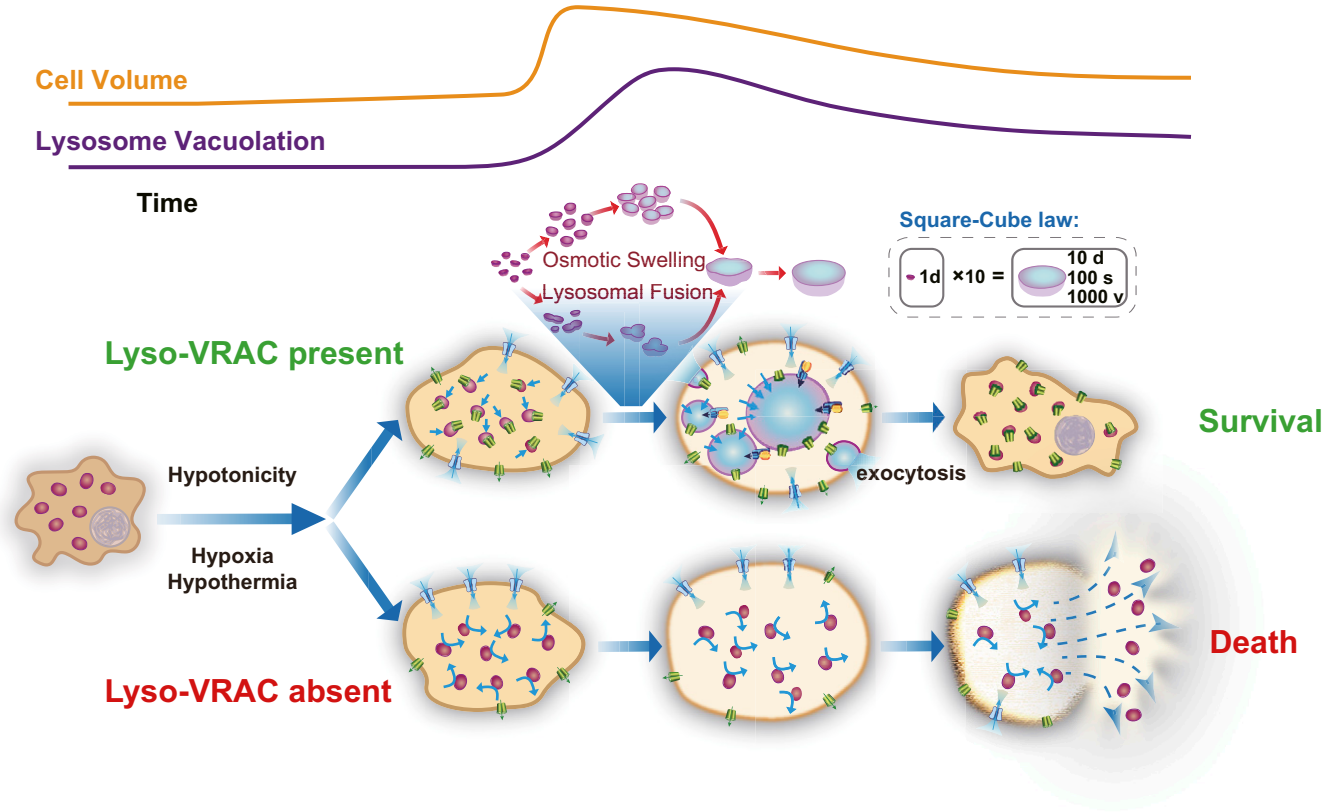

Fig. 7. Working model for how Lyso-VRAC–mediated lysosome osmoregulation behavior is protective for cell survival. Hypotonicity results in water influx through aquaporin channels on the plasma membrane (cyan), and the cell volume increases almost instantly (the yellow curve on the top). This decreases cytosolic ionic strength, normally activating VRAC channels (green) formed from LRRC8 proteins on both the plasma membrane (PM-VRAC) and in lysosomes (Lyso-VRAC). The activation of Lyso-VRAC (but not PM-VRAC) triggers lysosomal vacuolation (the purple curve on the top) through lysosomal osmotic swelling and/or homotypic fusion, creating large-volume compartments for intracellular water storage. Lysosome vacuolation decreases the cytosol volume of cells, helping to maintain the physiological concentrations of proteins and metabolites. Exocytosis of water-filled vacuoles substantially reduces the cell volume by dumping excess water into the extracellular environment and reduces plasma membrane tension stress by delivering more intracellular lipids to the cell surface (Survival, upper scenario). When Lyso-VRAC is absent, giant vacuoles do not form, the plasma membrane breaks, and cells die, even if PM-VRAC currents are normal (Death, lower scenario).

the osmotically active constituents cannot flow out so swelling occurs until the luminal osmotic strength matches the diluted cytosol. Consistent with the idea that Lyso-VRAC regulates water permeation as well as ion permeation, isolated WT lysosomes lyse much more rapidly in response to hypotonic solution (which would open Lyso-VRAC channels) than lysosomes from Lyso-VRAC–deficient cells. This demonstrates that Lyso-VRAC directly or indirectly controls water flux across the lysosomal membrane without the need for any factors normally present in the cytosol. Furthermore, this mechanism would explain why vacuolation can occur when PM-VRACs are blocked with NS3728 as water influx across the plasma membrane appears to be meditated by aquaporins, not by VRACs.

It is well known that lysosomes are the cell's center for degrading macromolecules. The amino acids and sugars produced by this catabolism contribute to luminal osmolarity, and lysosomal degradation itself is a water-consuming process (20). Thus, lysosomes are an excellent location to regulate intracellular water homeostasis and maintain osmotic homeostasis. The "bladder" function of lysosomes may therefore be fundamental and critical for cell survival under various physiological and pathological osmotic perturbations. The osmoregulatory role of lysosomes also could provide protection from cell damage in patients with hyponatremia, nephrotic syndrome, and liver cirrhosis (48). In addition to the hypotonic challenges present in the digestive tract and the collecting tubules of the kidney of adult animals, there are developmental challenges. The yolk sac and amniotic and allantoic fluid are all hypoosmotic to the developing fetus and may take on a level as low as 30 mOsm (49). Thus powerful osmoregulatory mechanisms are required to allow normal embryonic development (50). A role for Lyso-VRAC in this osmoregulatory behavior might account for some of the development deficiencies of LRRC8A knockout animals (51, 52). As Lyso-VRAC also protects cells from necrotic death caused by hypoxia and hypothermia, our identification of Lyso-VRAC provides a molecular foundation upon which to explore new links between lysosome function, normal human physiology, and disease pathologies.

Materials and Methods

Tissue culture, imaging, electrophysiology, biochemistry and molecular biology experiments, and statistical analysis were carried out using standard

methods. Additional information is provided in *SI Appendix, Supplemental Materials and Methods*.

Data Availability. All study data are included in the article, *SI Appendix*, and Movies S1–S4.

ACKNOWLEDGMENTS. This work was supported by NIH Grants NS062792 (to H.X.), DK115471 (to H.X. and R.I.H.), and AI039657 (to T.L.C.), and Department of Health and Human Services/National Cancer Institute Cancer Center Support Grant to MD Anderson Cancer Center (P30 CA016672) (to F.B.). Additional support was provided by an M-Cubed grant and a Protein Folding Disease Initiative grant from the University of Michigan (to H.X.). P.L. and M.H. performed experiments at the University of Michigan as visiting scholars from the Collaborative Innovation Center of Yangtze River Delta Region Green Pharmaceuticals. The funders had no role in study design, data collection and analysis, decision to publish, or preparation of the manuscript. We are grateful to Drs. Bo Duan, Laura Buttitta, and Cunming Duan and their laboratory members for assistance; and Randy Stockbridge for comments on an earlier version of the manuscript. We appreciate the encouragement and helpful comments provided by our H.X. laboratory colleagues, especially Dr. Xiaoli Zhang.

1. E. Delpire, K. B. Gagnon, Water homeostasis and cell volume maintenance and regulation. *Curr. Top. Membr.* **81**, 3–52 (2018).
2. E. K. Hoffmann, I. H. Lambert, S. F. Pedersen, Physiology of cell volume regulation in vertebrates. *Physiol. Rev.* **89**, 193–277 (2009).
3. C. W. Bourque, Central mechanisms of osmosensation and systemic osmoregulation. *Nat. Rev. Neurosci.* **9**, 519–531 (2008).
4. D. Kültz, Cellular osmoregulation: Beyond ion transport and cell volume. *Zoology (Jena)* **104**, 198–208 (2001).
5. T. J. Jentsch, VRACs and other ion channels and transporters in the regulation of cell volume and beyond. *Nat. Rev. Mol. Cell Biol.* **17**, 293–307 (2016).
6. N. C. Gauthier, T. A. Masters, M. P. Sheetz, Mechanical feedback between membrane tension and dynamics. *Trends Cell Biol.* **22**, 527–535 (2012).
7. D. Raucher, M. P. Sheetz, Characteristics of a membrane reservoir buffering membrane tension. *Biophys. J.* **77**, 1992–2002 (1999).
8. A. Diz-Muñoz, D. A. Fletcher, O. D. Weiner, Use the force: Membrane tension as an organizer of cell shape and motility. *Trends Cell Biol.* **23**, 47–53 (2013).
9. N. Groulx, F. Boudreault, S. N. Orlov, R. Grygorczyk, Membrane reserves and hypotonic cell swelling. *J. Membr. Biol.* **214**, 43–56 (2006).
10. E. S. Snigirevskaya, Y. Y. Komissarchik, Structural correlates of the transepithelial water transport. *Int. Rev. Cytol.* **198**, 203–275 (2000).
11. B. Bailey, K. L. Kirk, Diffusion resistances between ADH-induced vacuoles and the extracellular space in rabbit collecting duct: Evidence that most vacuoles are intracellular, endocytic compartments. *Cell Tissue Res.* **263**, 165–171 (1991).
12. J. B. Lloyd, S. Forster, The lysosome membrane. *Trends Biochem. Sci.* **11**, 365–368 (1986).
13. R. D. Park, P. C. Sullivan, B. Storrie, Hypertonic sucrose inhibition of endocytic transport suggests multiple early endocytic compartments. *J. Cell. Physiol.* **135**, 443–450 (1988).
14. D. Deneka, M. Sawicka, A. K. M. Lam, C. Paulino, R. Dutzler, Structure of a volume-regulated anion channel of the LRRC8 family. *Nature* **558**, 254–259 (2018).
15. F. K. Voss *et al.*, Identification of LRRC8 heteromers as an essential component of the volume-regulated anion channel VRAC. *Science* **344**, 634–638 (2014).
16. Z. Qiu *et al.*, SWELL1, a plasma membrane protein, is an essential component of volume-regulated anion channel. *Cell* **157**, 447–458 (2014).
17. R. Syeda *et al.*, LRRC8 proteins form volume-regulated anion channels that sense ionic strength. *Cell* **164**, 499–511 (2016).
18. J. M. Sands, H. E. Layton, Advances in understanding the urine-concentrating mechanism. *Annu. Rev. Physiol.* **76**, 387–409 (2014).
19. K. L. Kirk, Origin of ADH-induced vacuoles in rabbit cortical collecting tubule. *Am. J. Physiol.* **254**, F719–F733 (1988).
20. H. Xu, D. Ren, Lysosomal physiology. *Annu. Rev. Physiol.* **77**, 57–80 (2015).
21. P. Li, M. Gu, H. Xu, Lysosomal ion channels as decoders of cellular signals. *Trends Biochem. Sci.* **44**, 110–124 (2019).
22. D. E. Johnson, P. Ostrowski, V. Jaumouillé, S. Grinstein, The position of lysosomes within the cell determines their luminal pH. *J. Cell Biol.* **212**, 677–692 (2016).
23. S. A. Freeman *et al.*, Lipid-gated monovalent ion fluxes regulate endocytic traffic and support immune surveillance. *Science* **367**, 301–305 (2020).
24. L. Minieri *et al.*, The inhibitor of volume-regulated anion channels DCPIB activates TREK potassium channels in cultured astrocytes. *Br. J. Pharmacol.* **168**, 1240–1254 (2013).
25. D. M. Kern, S. Oh, R. K. Hite, S. G. Brohawn, Cryo-EM structures of the DCPIB-inhibited volume-regulated anion channel LRRC8A in lipid nanodiscs. *eLife* **8**, e42636 (2019).
26. B. Nilius, J. Prenen, T. Voets, J. Eggermont, G. Droogmans, Activation of volume-regulated chloride currents by reduction of intracellular ionic strength in bovine endothelial cells. *J. Physiol.* **506**, 353–361 (1998).
27. X. P. Dong *et al.*, The type IV mucolipidosis-associated protein TRPML1 is an endolysosomal iron release channel. *Nature* **455**, 992–996 (2008).
28. O. A. Brady, Y. Zheng, K. Murphy, M. Huang, F. Hu, The frontotemporal lobar degeneration risk factor, TMEM106B, regulates lysosomal morphology and function. *Hum. Mol. Genet.* **22**, 685–695 (2013).
29. R. Planells-Cases *et al.*, Subunit composition of VRAC channels determines substrate specificity and cellular resistance to Pt-based anti-cancer drugs. *EMBO J.* **34**, 2993–3008 (2015).
30. A. C. Komor, A. H. Badran, D. R. Liu, CRISPR-based technologies for the manipulation of eukaryotic genomes. *Cell* **168**, 20–36 (2017).
31. C. D. Platt *et al.*, Leucine-rich repeat containing 8A (LRRC8A)-dependent volume-regulated anion channel activity is dispensable for T-cell development and function. *J Allergy Clin Immunol* **140**, 1651–1659.e1, 10.1016/j.jaci.2016.12.974 (2017).
32. D. Lutter, F. Ullrich, J. C. Lueck, S. Kempa, T. J. Jentsch, Selective transport of neurotransmitters and modulators by distinct volume-regulated LRRC8 anion channels. *J. Cell Sci.* **130**, 1122–1133 (2017).
33. M. Abu-Remaileh *et al.*, Lysosomal metabolomics reveals V-ATPase- and mTOR-dependent regulation of amino acid efflux from lysosomes. *Science* **358**, 807–813 (2017).
34. W. Hunziker, H. J. Geuze, Intracellular trafficking of lysosomal membrane proteins. *Bioessays* **18**, 379–389 (1996).
35. T. L. Cover, S. R. Blanke, Helicobacter pylori VacA, a paradigm for toxin multifunctionality. *Nat. Rev. Microbiol.* **3**, 320–332 (2005).
36. N. Hélix, D. Strøbaek, B. H. Dahl, P. Christophersen, Inhibition of the endogenous volume-regulated anion channel (VRAC) in HEK293 cells by acidic di-aryl-ureas. *J. Membr. Biol.* **196**, 83–94 (2003).
37. T. K. Klausen *et al.*, Cell cycle-dependent activity of the volume- and Ca2+-activated anion currents in Ehrlich lettre ascites cells. *J. Cell. Physiol.* **210**, 831–842 (2007).
38. J. A. Mindell, Lysosomal acidification mechanisms. *Annu. Rev. Physiol.* **74**, 69–86 (2012).
39. L. S. King, D. Kozono, P. Agre, From structure to disease: The evolving tale of aquaporin biology. *Nat. Rev. Mol. Cell Biol.* **5**, 687–698 (2004).
40. A. Chaurra, B. M. Gutzman, E. Taylor, P. C. Ackroyd, K. A. Christensen, Lucifer Yellow as a live cell fluorescent probe for imaging water transport in subcellular organelles. *Appl. Spectrosc.* **65**, 20–25 (2011).
41. S. Hamann *et al.*, Measurement of cell volume changes by fluorescence self-quenching. *J. Fluoresc.* **12**, 139–145 (2002).
42. C. Zhou *et al.*, Transfer of cGAMP into bystander cells via LRRC8 volume-regulated anion channels augments STING-mediated interferon responses and anti-viral immunity. *Immunity* **52**, 767–781.e6 (2020).
43. J. E. Capó-Aponte, P. Iserovich, P. S. Reinach, Characterization of regulatory volume behavior by fluorescence quenching in human corneal epithelial cells. *J. Membr. Biol.* **207**, 11–22 (2005).
44. B. E. Steinberg *et al.*, A cation counterflux supports lysosomal acidification. *J. Cell Biol.* **189**, 1171–1186 (2010).
45. C. Cang *et al.*, mTOR regulates lysosomal ATP-sensitive two-pore Na(+) channels to adapt to metabolic state. *Cell* **152**, 778–790 (2013).
46. X. Wang *et al.*, TPC proteins are phosphoinositide- activated sodium-selective ion channels in endosomes and lysosomes. *Cell* **151**, 372–383 (2012).
47. B. Nilius, Is the volume-regulated anion channel VRAC a "water-permeable" channel? *Neurochem. Res.* **29**, 3–8 (2004).
48. M. M. Shah, P. Magdiga, *Physiology, Plasma Osmolality and Oncoic Pressure* (StatPearls, 2019).
49. M. H. Goldstein, F. W. Bazer, D. H. Barron, Characterization of changes in volume, osmolarity and electrolyte composition of porcine fetal fluids during gestation. *Biol. Reprod.* **22**, 1168–1180 (1980).
50. G. K. Baggott, Development of extra-embryonic membranes and fluid compartments. *Avian Biol. Res.* **2**, 21–26 (2009).
51. T. Yamada, R. Wondergem, R. Morrison, V. P. Yin, K. Strange, Leucine-rich repeat containing protein LRRC8A is essential for swelling-activated Cl- currents and embryonic development in zebrafish. *Physiol. Rep.* **4**, e12940 (2016).
52. L. Kumar *et al.*, Leucine-rich repeat containing 8A (LRRC8A) is essential for T lymphocyte development and function. *J. Exp. Med.* **211**, 929–942 (2014).